**Mathematical Modelling and Numerical Analysis** ESAIM: M2AN
Modélisation Mathématique et Analyse Numérique Vol. 34, N° 6, 2000, pp. 1123–1149

# CONVERGENCE RATE OF A FINITE VOLUME SCHEME FOR THE LINEAR CONVECTION-DIFFUSION EQUATION ON LOCALLY REFINED MESHES

Yves Coudière[1] and Philippe Villedieu[2]

**Abstract.** We study a finite volume method, used to approximate the solution of the linear two dimensional convection diffusion equation, with mixed Dirichlet and Neumann boundary conditions, on Cartesian meshes refined by an automatic technique (which leads to meshes with hanging nodes). We propose an analysis through a discrete variational approach, in a discrete $H^1$ finite volume space. We actually prove the convergence of the scheme in a discrete $H^1$ norm, with an error estimate of order $O(h)$ (on meshes of size $h$).

**Mathematics Subject Classification.** 65C20, 65N12, 65N15, 76R50, 45L10.

Received: October 19, 1999. Revised: June 28, 2000.

## 1. Introduction

Consider the following two dimensional mixed boundary value problem: find $u$ in $H^2(\Omega)$, such that

$$\operatorname{div}(-\nu\nabla u + u\mathbf{v}) = f, \quad \text{on } \Omega, \qquad \left| \begin{array}{rcl} u_{|\Gamma^D} & = & g, \\ \partial_{\mathbf{n}_{ext}} u_{|\Gamma^N} & = & k. \end{array} \right. \tag{1}$$

$\nu \geq \nu_0 > 0$ and $\mathbf{v} = (\mathbf{v}_x, \mathbf{v}_y)$ are given parameters. $f$, $g$, and $k$ are given functions. $(\Gamma^D, \Gamma^N)$ is a partition of $\partial\Omega$ ($\Omega \subset \mathbb{R}^2$).

Equation (1) is a simplified model of many problems of computational physics (fluid flows, heat transfer, pollutant dispersion, reservoir simulation, ...), for which finite volume are widely used. Given a partition of $\Omega$ into some polyhedral cells $K$, called *control volumes*, the approximation is a function piecewise constant on the control volumes (cell centered approach). The idea of finite volume schemes is to discretize the integral of (1) on the control volumes (one equation for one unknown). Hence, using Green's formula, the problem reduces to approximating some fluxes along the interfaces between the control volumes.

The discretization of the flux of convection has been widely studied during the last twenty years, even for non linear equations. Unstructured meshes are usually treated, and mesh refinement becomes a usual technique in the approximation of non linear hyperbolic problems.

*Keywords and phrases.* Finite volumes, mesh refinement, convection-diffusion, convergence rate.

[1] Mathématiques pour l'Industrie et la Physique, UMR 5640, INSA, 135 avenue de Rangueil, 31077 Toulouse Cedex 4, France. e-mail: Yves.Coudiere@sophia.inria.fr

[2] ONERA, Centre de Toulouse, 2 avenue Ed. Belin, 31055 Toulouse Cedex 4, France. e-mail: Philippe.Villedieu@cert.fr

Our aim is to describe, and analyze some techniques of discretization for the viscous flux (flux of $\nabla u \cdot \mathbf{n}$) on *unstructured meshes, with local refinement*. We are specially interested in an Automatic Mesh Refinement technique (AMR technique, Fig. 1) [3, 7].

The main issues of this paper are:

- finding an accurate and stable method in order to approximate the derivatives of the piecewise constant approximation, on Cartesian meshes, locally refined by an AMR technique;
- analyzing the convergence of the resulting scheme, and giving some error estimates.

The convergence of finite volume schemes has been initially studied by Manteuffel and White [22], Weiser and Wheeler [31], Heinrich [17], and Forsyth and Sammon [16]. The results of these authors concerns non uniform Cartesian meshes, but they contains the main ideas of lots of subsequent developments:

- finite volume schemes are not consistent in the sense of finite differences (Taylor expansions), the theorem of Lax is useless in this context;
- two different techniques may be applied to study their convergence;
  - the mesh of the control volume can be considered as the geometrical dual of a mesh which defines a $H^1$ conformal finite elements space (for instance $P_1$, or $Q_1$);
  - the scheme is seen as a mixed finite element scheme, with an appropriate numerical integration;

  In both cases, finite element techniques are used, and a $H^1$ error estimate of order $O(h)$ (for meshes of size $h$) is proved.

Some authors have developed the first approach, either on Cartesian meshes [25, 26], or on unstructured meshes [1, 4–6, 23]. The most recent result is the convergence of the finite volume element method of Cai [4] for general elliptic equations of the form $-\mathrm{div}\,(A\nabla u) = f$ for any positive matrix $A$ [20].

The second approach has been studied by Baranger *et al.* [2], Courbet and Croisille [12], and Thomas and Trujillo [27, 28], using different conforming or non-conforming finite element spaces and different numerical integrations.

An explicit calculation of the matrix of the discrete problem yields some results on composite Cartesian grids and composite grids of equilateral triangles [14, 30].

Another approach is due to R. Herbin, who proved an error estimate of order $O(h)$ in a discrete $H^1$ norm, on meshes of triangles, but with a different analysis, of finite volume type [18]. It has been extended to a more general class of meshes [15], which are defined by the following restrictions: the line joining the centers of two neighboring control volume must be perpendicular to the interface between the control volume. In that case, the difference between the values of the approximation on two neighboring control volume is a consistent approximation of $\nabla u \cdot \mathbf{n}$ on the interface. Similar results for Voronoï meshes (which are of the previous class) can be found in [24]. And a finite element interpretation has been given [29].

But meshes refined by AMR techniques cannot in general be treated as standard finite element ones, nor do they belong to the class of meshes mentioned above. Several methods has been proposed to approximate the derivatives in that case [7, 8, 19]. They are based on the construction of an interpolation of the approximation. Here, we choose the so-called *diamond path* technique [7], that consists in interpolating some values at the vertices of the mesh: theses values allow the construction of discrete tangential derivatives. It is a very simple method, that seems to be robust [7], and that can be extended to arbitrary meshes.

A general framework to analyze the scheme obtained by this method has been introduced in a joint work of the authors with Vila [11]. It is derived from the analysis introduced by Herbin [18]. The main ideas are the following [9]:

- introduce a discrete variational problem, on the (non conforming) space of the piecewise constant functions;
- introduce a discrete $H_0^1$ semi norm, which appears in a discrete integration by parts;
- verify that the discrete $H_0^1$ semi norm is a norm (discrete inequality of Poincaré), and consider then the space of the piecewise constant functions as a discrete version of $H^1$;
- prove then the consistency of the scheme in a variational sense, which is also the consistency of the numerical fluxes;
- prove the coercivity of the discrete variational form, with respect to the discrete $H^1$ semi norm.

Finally, following this procedure, we obtain an error estimate of order $O(h)$ (on meshes of size $h$), in the discrete $H^1$ norm. Although it would not be detailed here, it can be proved some discrete inequalities of Sobolev for our discrete norm, which permits to give some error estimates in $L^p$ norms ($1 \leq p \leq +\infty$) [10].

On general meshes, which just verify some classical hypotheses of non local degeneracy, the inequality of Poincaré is true (it is independent from the scheme [9]), and the consistency is easily obtained, via some hypotheses on the local interpolations at the vertices of the mesh (see the previous work [11]).

The coercivity is the main difficulty. It has been proved for meshes of quadrangles [11]. Here, we prove that:

- the coercivity is a local property (around the vertices) of the geometry of the mesh and of the interpolation weights,
- it does not depend on the size of the mesh, but on its aspect.

The local coercivity is found by calculating the eigenvalues of a small symmetric matrix (of size the number of neighbors of the concerned vertex).

Although this problem may be numerically solved on any mesh, we could actually solve it analytically only for Cartesian meshes of rectangles, refined by an AMR technique (so called *locally refined Cartesian meshes*).

Hence, the finite volume approximation $u_h$ defined by the *diamond path* method converges to the exact solution $u$ on a family of *locally refined Cartesian meshes* of sizes $h$, with the error estimates

$$\|u - u_h\|_{L^2(\Omega)} + |u - u_h|_{1,h} \leq c\, h,$$

supposing that $u \in H^2(\Omega)$.

We present here the scheme on locally refined Cartesian meshes (Sect. 2), a summarized analysis in general (Sect. 3) and the consistency and coercivity only on locally refined Cartesian meshes (Sects. 4 and 5).

For sake of simplicity, we shall suppose that $\nu \in \mathbb{R}$ is constant, as well as $\mathbf{v} \in \mathbb{R}^2$, and that $f$, $g$, $k$, and $\Omega$ are regular enough for the exact solution $u$ to belong to $H^2(\Omega)$ (for example $\Omega$ convex and polygonal, $f \in L^2(\Omega)$ for Dirichlet boundary conditions [13]).

## 2. The numerical scheme

### 2.1. Locally refined Cartesian meshes

We consider meshes of rectangles (Fig. 1) with constant step-sizes, $\Delta x$ and $\Delta y$. Each rectangle may be divided into four similar rectangles. The resulting meshes are called *"Cartesian and locally refined"*. They shall verify the following hypotheses.

**Hypothesis 2.1** (Regularity assumptions)**.**

- There is at most one step of refinement between two neighboring cells.
- The number of steps of refinement between the largest rectangle and the smallest one is bounded.

We shall denote by $T_h$ a mesh which larger rectangle is of size $h$ (*i.e.* $h = \max(\Delta x, \Delta y)$).

### 2.2. The finite volume scheme

The elements (rectangles) of a mesh $T_h$ are called *control volumes*, and denoted by $K$. The finite volume discretization of (1) consists in introducing a piecewise constant approximation of $u$, denoted by $u_h$, and defined as

$$\forall x \in K, \qquad u_h(x) = u_K.$$

The values of $u_h$ are calculated according to the following scheme:

$$\sum_{e \in \partial K} s_{Ke} \left(\phi_e^D(u_h) + \phi_e^C(u_h)\right) m(e) = f_K m(K), \tag{2}$$

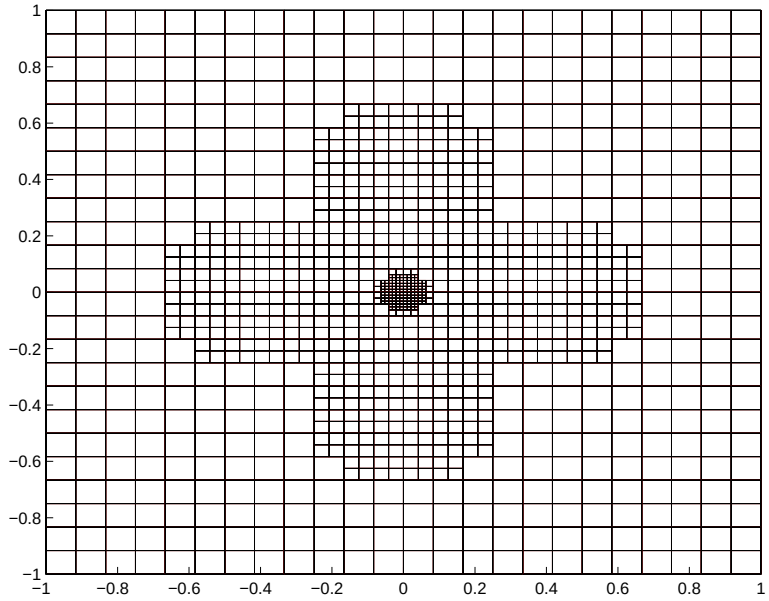


FIGURE 1. Example of a Mesh.

which is a discretization of the integral equation

$$\int_{\partial K} (-\nu \nabla u + u\mathbf{v}) \cdot \mathbf{n}_{\text{ext}} \, \mathrm{d}\sigma \; = \; \int_K f \, \mathrm{d}x.$$

$\partial K$ denotes the boundary of $K$, constituted of the edges $e$, which may be, either interfaces between $K$ and another cell, or boundary edges, of type Neumann or Dirichlet.

**Notation 2.1** (Interfaces)**.** We shall denote by

- $S_h^\star$ the set of the interfaces (*i.e.* the interior edges);
- $\partial S_h$ (resp. $\partial S_h^{N/D}$) the set of the boundary edges (resp. of Neumann/Dirichlet type);

and $S_h = S_h^\star \cup \partial S_h$.

$f_K$ is the mean value of $f$ on $K$:

$$f_K = \frac{1}{m(K)} \int_K f \, \mathrm{d}x.$$

$m(K)$ and $m(e)$ are, respectively, the measure in $\mathbb{R}^2$ of $K$, and the measure in $\mathbb{R}$ of $e$. $\phi_e^D(u_h)$ (approximation of $-\dfrac{1}{m(e)} \displaystyle\int_e \nu \nabla u_h \cdot \mathbf{n}_{\text{ext}} \mathrm{d}\sigma$) and $\phi_e^C(u_h)$ (approximation of $\dfrac{1}{m(e)} \displaystyle\int_e u_h \mathbf{v} \cdot \mathbf{n}_{\text{ext}} \mathrm{d}\sigma$) are the average numerical fluxes of diffusion and convection along $e$, in the direction of a unit normal to $e$, $\mathbf{n}_e$, chosen *a priori*.

**Notation 2.2** (*A priori* orientation of the interfaces)**.** Any edge $e \in S_h$ is oriented *a priori* by a unit normal $\mathbf{n}_e$. In order to simplify the expression of the flux of convection, $\mathbf{n}_e$ is taken such that

$$\mathbf{v} \cdot \mathbf{n}_e \geq 0$$

(if $\mathbf{v} \cdot \mathbf{n}_e = 0$ then the direction of $\mathbf{n}_e$ does not matter). We denote by:

- $W$ the upstream control volume (if it exists), with respect to $\mathbf{n}_e$;
- $E$ the downstream control volume (if it exists), with respect to $\mathbf{n}_e$.

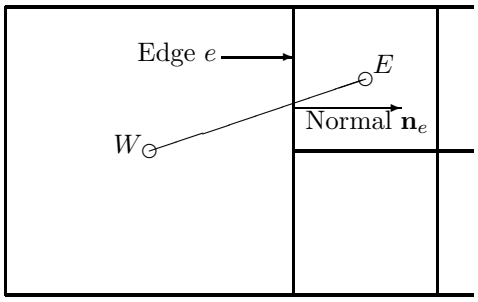


FIGURE 2. Orientation of an interface.

Consequently, $s_{Ke} = 1$ if $\mathbf{n}_e$ is the unit normal outward to $K$, and $s_{Ke} = -1$ otherwise. The fluxes are defined in the following paragraphs.

## 2.3. The flux of convection

We take the simple first order upwind scheme, in order to approximate $u_h \mathbf{v} \cdot \mathbf{n}_e$ along $e$:

$$\forall e \in S_h^\star, \quad \phi_e^C(u_h) = \mathbf{v} \cdot \mathbf{n}_e u_W, \quad \text{since } \mathbf{v} \cdot \mathbf{n}_e \geq 0, \tag{3}$$

$$\forall e \in \partial S_h, \quad \phi_e^C(u_h) = \left| \begin{array}{l} \mathbf{v} \cdot \mathbf{n}_e u_W, \quad \text{if } s_{Ke} = 1 \\ \mathbf{v} \cdot \mathbf{n}_e g(x_e), \quad \text{if } s_{Ke} = -1 \end{array} \right. \tag{4}$$

(assuming that $x_e$ is the midpoint of $e$).

## 2.4. The flux of diffusion

$\phi_e^D(u_h)$ should be an approximation of $-\nu \nabla u_h \cdot \mathbf{n}_e$, but $u_h$ is not differentiable. Consequently, we shall use some discrete derivatives.

**Notation 2.3** (Geometry around an interface, Fig. 3)**.** We denote by:

- $x_K$ the center of gravity of the control volume $K$;
- for an edge $e \in S_h$,
  - $\mathbf{t}_e$ the unit tangent to $e$, such that $(\mathbf{n}_e, \mathbf{t}_e)$ is a direct basis,
  - $x_N$ and $x_S$ the endpoints of $e$ such that

$$(x_N - x_S) \cdot \mathbf{t}_e > 0;$$

  - $h_e$ the distance

$$h_e = (x_E - x_W) \cdot \mathbf{n}_e,$$

    - if $e \in \partial S_h$ and $\mathbf{n}_e$ is outward to $\Omega$, $x_E$ denotes the midpoint of $e$, $x_e$,
    - if $e \in \partial S_h$ and $\mathbf{n}_e$ is inward to $\Omega$, $x_W$ denotes the midpoint of $e$, $x_e$.

Along the edges which does not intersect the Neumann boundary,

- $\nabla u_h \cdot (x_E - x_W)$ is approximated by $u_E - u_W$,
- $\nabla u_h \cdot (x_N - x_S)$ is approximated by $u_N - u_S$, for some suitable interpolated values $u_N$ and $u_S$ at the vertices $N$ and $S$ (see Sect. 2.5).

Consequently, the flux of diffusion shall involve the angle between the direction $x_E - x_W$ and the direction normal to $e$.

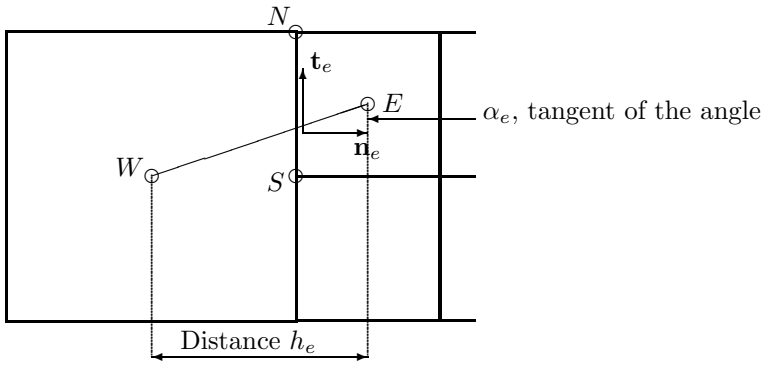


FIGURE 3. Geometry around an interface.

**Notation 2.4** (Angle $\alpha_e$)**.** For any edge $e \in S_h$, we denote by $\alpha_e$ the tangent

$$\alpha_e = \frac{(x_E - x_W)\cdot \mathbf{t}_e}{(x_E - x_W)\cdot \mathbf{n}_e}.$$

$\alpha_e$ is actually 0 if $E$ and $W$ have the same size, and $\pm\dfrac{\Delta x}{3\Delta y}$ (horizontal edges) or $\pm\dfrac{\Delta y}{3\Delta x}$ (vertical edges) otherwise.

Finally, the flux of diffusion is

$$\phi_e^D(u_h) \;=\; -\nu\left(\frac{u_E - u_W}{h_e} \;-\; \alpha_e \frac{u_N - u_S}{m(e)}\right). \tag{5}$$

Along the edges of the Neumann boundary ($e \in \partial S_h^N$), we naturally take

$$\phi_e^D(u_h) \;=\; \frac{1}{m(e)}\int_e k\,\mathrm{d}\sigma. \tag{6}$$

Along the interior edges which intersect the Neumann boundary ($e \in S_h^\star$, $\mid \bar{e} \cap \Gamma^N \neq \emptyset$), $u_E - u_W$ still approximates $\nabla u_h \cdot (x_E - x_W)$, while $\nabla u_h \cdot \mathbf{t}_e$ is approximated by:

- using the interpolated value at the interior endpoint of $e$;
- using the Neumann boundary condition at the boundary endpoint of $e$.

We find that, if $x_N$ is the boundary vertex (Fig. 4),

$$\phi_e^D(u_h) \;=\; -\nu\left(\frac{u_E - u_W}{h_e} \;-\; \alpha_e\left(\frac{|x_N - x_e|k_N + u_e - u_S}{m(e)}\right)\right), \tag{7}$$

otherwise ($x_S$ is the boundary vertex),

$$\phi_e^D(u_h) \;=\; -\nu\left(\frac{u_E - u_W}{h_e} \;-\; \alpha_e\left(\frac{u_N - u_e + |x_e - x_S|k_S}{m(e)}\right)\right). \tag{8}$$

$x_e$ is the intersection of $e$ and $[x_E, x_W]$. $u_e$ is a value interpolated linearly at $x_e$, from $u_E$ and $u_W$:

$$u_e = \frac{h_e^W u_E + h_e^E u_W}{h_e}, \text{ where } h_e^W \;=\; (x_S - x_W)\cdot \mathbf{n}_e \text{ and } h_e^E \;=\; (x_E - x_S)\cdot \mathbf{n}_e.$$

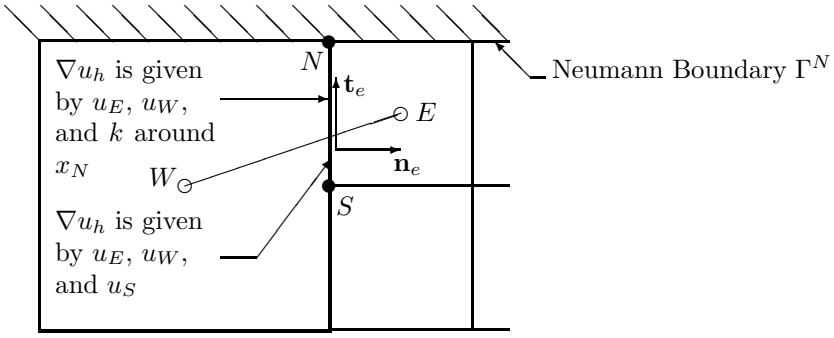


FIGURE 4. Interface near the Neumann boundary.

$k_N$ (resp. $k_S$) is the average value of $k$ on the boundary $\Gamma^N$, around $x_N$ (resp. $x_S$):

$$k_{N\,(\text{resp. } S)} = \frac{1}{m(\gamma)} \int_\gamma k \, \mathrm{d}\sigma, \text{ where } \gamma = \Gamma^N \cap (E \cup W)\,.$$

## 2.5. **The interpolation**

**Notation 2.5** (Notations around a vertex)**.** We shall denote by:

- $\mathcal{N}_h^\star$ the set of the vertices interior to $\Omega$;
- $\partial\mathcal{N}_h$ (resp. $\partial\mathcal{N}_h^{N/D}$) the set of the vertices on the boundary of $\Omega$ (resp. of type Neumann/Dirichlet);

and $\mathcal{N}_h = \mathcal{N}_h^\star \cup \partial\mathcal{N}_h$.

For a given vertex $M \in \mathcal{N}_h \backslash \partial\mathcal{N}_h^N$ we also denote by $\mathcal{V}_M$ the set of the control volumes $K$ that share the vertex $M$.

For the interior vertices, $M \in \mathcal{N}_h^\star$, we take

$$u_M = \sum_{K \in \mathcal{V}_M} y_K(M) u_K,$$

where the $(y_K(M))_{K\in\mathcal{V}_M}$ are suitable *weights of interpolation around* $M$.

For the vertices of the Dirichlet boundary, $M \in \partial\mathcal{N}_h^D$, we take

$$u_M = g(x_M).$$

# 3. SUMMARIZED ANALYSIS

## 3.1. **Principle**

Given the boundary conditions $g$ and $k$, consider the discrete operator defined on the functions $u_h$ piecewise constant on $T_h$ by

$$\mathcal{L}_h u_h = \mathcal{L}_h^D u_h + \mathcal{L}_h^C u_h,$$

where

$$\mathcal{L}_h^D\, u_h = \left\{ \frac{1}{m(K)} \sum_{e\in\partial K} s_{Ke}\, \phi_e^D(u_h)\, m(e) \right\}_{K\in T_h}$$

$$\mathcal{L}_h^C\, u_h = \left\{ \frac{1}{m(K)} \sum_{e\in\partial K} s_{Ke}\, \phi_e^C(u_h)\, m(e) \right\}_{K\in T_h}$$

where the numerical fluxes are defined by (3) to (8). This operator is not consistent in general (in the sense of finite differences, see [17, 22]). Hence we shall consider the bilinear form:

$$a_h(u_h,\, v_h) \,=\, (\mathcal{L}_h\, u_h,\, v_h)_{L^2(\Omega)}\,,$$

*defined on the functions piecewise constant.* The discrete problem is

$$\mathcal{L}_h\, u_h \,=\, f_h, \quad \text{or} \quad a_h(u_h,\, v_h) \,=\, (f,\, v_h)_{L^2(\Omega)} \quad (\forall v_h \text{ piecewise constant}).$$

The difference with a conformal finite element scheme is the following: $u_h$ and $v_h$ are only piecewise constant functions, and $a_h$ is defined only for such functions. $\mathcal{L}$ being the exact operator ($\mathcal{L}u = \operatorname{div}(u\mathbf{v} - \nu\nabla u)$), we consider the bilinear form

$$a(u, v) \,=\, (\mathcal{L}u,\, v)_{L^2(\Omega)}$$

defined on $H^2(\Omega)\times L^2(\Omega)$. The exact solution verifies

$$a(u,\, v_h) \,=\, (f,\, v_h)_{L^2(\Omega)} \quad (\forall v_h \text{ piecewise constant}),$$

and then we have

$$a_h(u_h,\, v_h) \,=\, a(u,\, v_h) \quad (\forall v_h \text{ piecewise constant}).$$

$\bar{u}_h$ being the piecewise constant $L^2$-perpendicular projection of $u$, and taking $v_h \,=\, u_h - \bar{u}_h$ as a test function, we get:

$$a_h(u_h - \bar{u}_h,\, u_h - \bar{u}_h) \,=\, a(u,\, u_h - \bar{u}_h) \,-\, a_h(\bar{u}_h,\, u_h - \bar{u}_h).$$

Remark that $a_h$ is defined on the space of the piecewise constant functions. We shall define a discrete $H_1$ semi-norm, such that the space of the piecewise constant functions becomes a discretization of the space $H^1(\Omega)$. Hence, the convergence involves the coercivity of $a_h$ (in the discrete $H_1$ norm), and its consistency (in the variational meaning).

### 3.2. **Consistency**

We shall see that the consistency of $a_h$ (variational consistency) is a consequence of the consistency of the numerical fluxes (in the sense of some Taylor expansions).

For $u \in H^2(\Omega)$, let $\bar{\phi}^D$ and $\bar{\phi}^C$ be the exact average fluxes:

$$\forall e \in S_h, \qquad \bar{\phi_e^C}(u) \,=\, \frac{1}{m(e)} \int_e u\mathbf{v}\cdot\mathbf{n}_e \,\mathrm{d}\sigma, \quad \bar{\phi_e^D}(u) = -\frac{1}{m(e)} \int_e \nu\nabla u\cdot\mathbf{n}_e \,\mathrm{d}\sigma.$$

Let $R_e(u) \,=\, \nu R_e^D(u) \,+\, (\mathbf{v}\cdot\mathbf{n}_e) R_e^C(u)$ be the error of consistency on the fluxes:

$$R_e^D(u) = \frac{1}{\nu}\left(\bar{\phi_e^D}(u) \,-\, \phi_e^D(\bar{u}_h)\right) \qquad R_e^C(u) = \frac{1}{m(e)} \int_e u\mathrm{d}\sigma \,-\, u\bar{_W}.$$

**Definition 3.1** (Consistency)**.** $\mathcal{L}_h$ is said to be consistent in $H^2$ on $(T_h)_{h>0}$ if there exists $c > 0$ such that $\forall u \in H^2(\Omega)$, such that $u_{|\Gamma^D} = g$ and $\partial_{\mathbf{n}} u_{|\Gamma^N} = k$,

$$\left( \sum_{e \in S_h \setminus \partial S_h^N} |R_e(u)|^2 m(e) h_e + 2 \sum_{e \in \partial S_h^N} |R_e^C(u)|^2 (\mathbf{v} \cdot \mathbf{n}_e) m(e) \right)^{1/2} \leq ch.$$

On the edges of the Neumann boundary ($e \in \partial S_h^N$), only the error on the flux of convection appears ($R_e^C(u)$), since the numerical flux of diffusion is exact ($\phi_e^D(\bar{u}_h) = \bar{\phi}_e^D(u)$).

The Definition 3.1 means that $a_h$ is consistent in the following sense: $\forall v_h$ piecewise constant, we have (after a discrete integration by parts)

$$|a(u, v_h) - a_h(\bar{u}_h, v_h)| \leq \sum_{e \in S_h \setminus \partial S_h^N} |R_e(u) \frac{v_E - v_W}{h_e}| m(e) h_e + \sum_{e \in \partial S_h^N} |R_e^C(u) v_W| (\mathbf{v} \cdot \mathbf{n}_e) m(e).$$

Now, using the inequality of Schwarz and assuming that the scheme is consistent (Def. 3.1), we find that, $\forall v_h$ piecewise constant,

$$\begin{aligned} |a(u, v_h) - a_h(\bar{u}_h, v_h)| &\leq c\, h \left( \sum_{e \in S_h \setminus \partial S_h^N} \left| \frac{v_E - v_W}{h_e} \right|^2 m(e) h_e + \frac{1}{2} \sum_{e \in \partial S_h^N} |v_W|^2 (\mathbf{v} \cdot \mathbf{n}_e) m(e) \right)^{1/2} \\ &= c\, h\, |v_h|_{1,h} \end{aligned}$$

where

$$|v_h|_{1,h}^2 = \sum_{e \in S_h \setminus \partial S_h^N} \left| \frac{v_E - v_W}{h_e} \right|^2 m(e) h_e + \frac{1}{2} \sum_{e \in \partial S_h^N} |v_W|^2 (\mathbf{v} \cdot \mathbf{n}_e) m(e), \tag{9}$$

noting $v_e = 0$ for any $e \in \partial S_h^D$.

### 3.3. **Coercivity**

We should use a property of coercivity in the following sense:

$$a_h(u_h - \bar{u}_h, u_h - \bar{u}_h) = (\mathcal{L}_h(u_h - \bar{u}_h), u_h - \bar{u}_h)_{L^2(\Omega)} \geq \text{cste}\, |u_h - \bar{u}_h|_{1,h}^2$$

(using the discrete $H^1$ semi-norm (9) defined above). Setting $v_h = u_h - \bar{u}_h$, $\mathcal{L}_h v_h$ is then defined by formulae (5–8), but taking $g = 0$ and $k = 0$.

**Definition 3.2** (Coercivity)**.** $\mathcal{L}_h$ is said to be coercive on $(T_h)_{h>0}$ if there exists $c^\star > 0$ such that $\forall h > 0$, and $\forall v_h$ piecewise constant,

$$a_h(v_h, v_h) = (\mathcal{L}_h v_h, v_h)_{L^2(\Omega)} \geq c^\star\, |v_h|_{1,h}^2$$

(taking the boundary conditions $g = 0$ and $k = 0$ to define $a_h$).

**Lemma 3.1.** *$\forall v_h$ piecewise constant,*

$$\left(\mathcal{L}_h^C v_h, v_h\right)_{L^2(\Omega)} \geq \frac{1}{2} \sum_{e \in \partial S_h^N} (\mathbf{v} \cdot \mathbf{n}_e) |v_W|^2\, m(e).$$

This is a natural consequence of our choice of an upwind scheme for the flux of convection.

**Theorem 3.1** (Inequality of Poincaré). *There exists $\omega$ such that $\forall h > 0$, $\forall v_h$,*

$$\|v_h\|_{L^2(\Omega)} \leq \omega\, |v_h|_{1,h}.$$

We refer to [9,15] for the proofs of Lemma 3.1 and Theorem 3.1.

### 3.4. **Convergence**

**Theorem 3.2** (Convergence). *If the discrete operator $\mathcal{L}_h$ is consistent (Def. 3.1) and coercive (Def. 3.2), then:*

- *for all $h > 0$, the discrete problem $\mathcal{L}_h u_h = f_h$ admits a unique solution $u_h$ piecewise constant;*
- *we have the following error estimate:*

$$|u_h - \bar{u}_h|_{1,h} + \|u_h - u\|_{L^2(\Omega)} \leq C\, h. \tag{10}$$

Indeed, in that case, we have, noting $\varepsilon_h = u_h - \bar{u}_h$,

$$c^\star |\varepsilon_h|^2_{1,h} \leq a_h(\varepsilon_h, \varepsilon_h) \leq |a(u, \varepsilon_h) - a_h(\bar{u}_h, \varepsilon_h)| \leq c|\varepsilon_h|_{1,h}\, h.$$

(10) is easily deduced from this inequality (and the inequality of Poincaré), with $C = \dfrac{c}{c^\star}(1+\omega)$.

## 4. Convergence of the finite volume scheme

The inequality of Poincaré is always true in general, under some regularity assumptions on the family of meshes $(T_h)_{h>0}$, which are satisfied here under Hypothesis 2.1.

The consistency and the coercivity of the scheme depend on the weights of the interpolation. The consistency is obtained easily, and we shall see that the coercivity is the main difficulty. We shall prove here that if the aspect ratio of the mesh verifies

$$\frac{1}{r} < \frac{\Delta x}{\Delta y} < r, \text{ where } r = 3 + 2\sqrt{2} \approx 5.8284,$$

then the scheme is coercive.

### 4.1. **The weights of the interpolation**

For sake of simplicity we may choose the weights now. Hence, let $M \in \mathcal{N}_h^\star$ be any interior vertex; and recall that $\mathcal{V}_M$ denotes the set of the cells that share $M$. For the piecewise constant function $u_h$, let $w$ be a function linear on $\mathcal{V}_M$ and such that

$$J(w) = \sum_{K \in \mathcal{V}_M} |w(x_K) - u_K|^2 \text{ is minimum among the linear functions.}$$

Finally, the solution $w$ depends linearly on the $u_K$ ($K \in \mathcal{V}_M$), and we can take

$$u_M = w(x_M) = \sum_{K \in \mathcal{V}_M} y_K(M) u_K.$$

Under Hypothesis 2.1, there are only a finite number of possible geometrical configurations. In each case, the weights are calculated according to this procedure. The results are summarized in Figure 5.

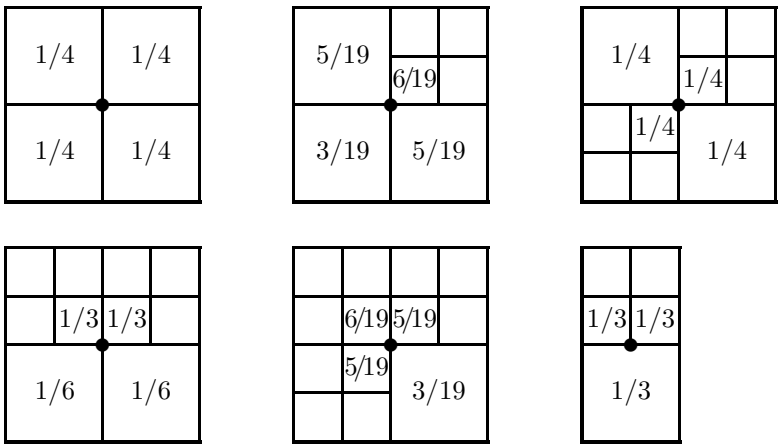


FIGURE 5. Summary of the geometrical situations, and weights.

## 4.2. **Consistency**

For any given edge $e \in S_h$ (interior or boundary), let

- $\Omega_e$ be the subset of $\Omega$ consisting of those control volumes $K$ that share a vertex with $e$:

$$\Omega_e = \cup \left\{ \bar{K} \mid N \in \bar{K}, \text{ or } S \in \bar{K} \right\};$$

- $R_e^D$ and $R_e^C$ be the functions defined by

$$u \in H^2(\Omega_e) \longrightarrow R_e^D(u) = -\frac{1}{m(e)} \int_e \nabla u \cdot \mathbf{n}_e \mathrm{d}\sigma - \frac{1}{\nu} \phi_e^D(\bar{u}_h),$$

$$u \in H^1(\Omega_e) \longrightarrow R_e^C(u) = \frac{1}{m(e)} \int_e u \mathrm{d}\sigma - \bar{u}_W,$$

where $\phi_e^D(\bar{u}_h)$ is given by (5), (6), (7), or (8), assuming that $g = u_{|\Gamma^D}$ and $k = \partial_{\mathbf{n}} u_{|\Gamma^N}$. We recall that $\bar{u}_h$ is the $L^2$ projection of $u$:

$$\bar{u}_K = \frac{1}{m(K)} \int_K u.$$

**Theorem 4.1** (Condition of consistency)**.** *Suppose that, for any edge $e \in S_h$,*

1. $R_e^D(u) = 0$ *for the linear functions,*
2. $R_e^C(u) = 0$ *for the constant functions,*

*then, the scheme is consistent in the sense of Definition 3.1.*

*Proof.*

**First step.** Consider $e \in S_h \backslash \partial S_h^N$. The local domain $\Omega_e$ is the image of a reference domain $\widehat{\Omega}$ (Fig. 6), and there are only a finite number of reference domains (including both interior and boundary cases). As a consequence, the main idea of the proof is to use the lemma of Bramble and Hilbert, in a classical way (see [21] for instance).

Since $h = \sup\{m(e)\}$, there exists $\bar{h} \leq h$ such that the transformation $x = \psi(\hat{x}) = x_S + \bar{h}\hat{x}$ maps a reference figure $\widehat{\Omega}$ into $\Omega_e$.

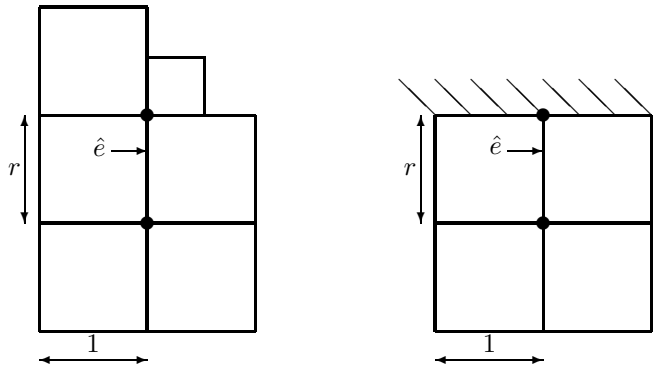


FIGURE 6. Examples of reference configurations $\widehat{\Omega}$.

On the reference figure $\widehat{\Omega}$, let $\widehat{R_e^D}$ and $\widehat{R_e^C}$ be the functions defined by

$$\hat{u} \in H^2(\widehat{\Omega}) \longrightarrow \widehat{R_e^D}(\hat{u}) = -\frac{1}{m(\hat{e})}\int_{\hat{e}} \nabla\hat{u}\cdot\widehat{\mathbf{n}}_e \mathrm{d}\sigma \; - \; \frac{1}{\nu}\widehat{\phi_e^D}(\bar{\hat{u}}) \text{ (which does not depend on } \nu),$$

$$\hat{u} \in H^1(\widehat{\Omega}) \longrightarrow \widehat{R_e^C}(\hat{u}) = \frac{1}{m(\hat{e})}\int_{\hat{e}} \hat{u}\mathrm{d}\sigma \; - \; \bar{\hat{u}}_W,$$

where $\hat{e} = \psi^{-1}(e)$.

$\widehat{\phi_e^D}(\hat{u})$ is given by formulae analog to (5–8); using the functions $\hat{g} = \hat{u}_{|\widehat{\Gamma^D}}$ and $\hat{k} = \partial_{\widehat{\mathbf{n}}}\hat{u}_{|\widehat{\Gamma^N}}$ if $\widehat{\Omega}$ takes into account a part of $\widehat{\Gamma} = \psi^{-1}(\Gamma)$, and where $\bar{\hat{u}}$ is the $L^2$ projection of $\hat{u}$, such that $\bar{\hat{u}}_{\hat{K}} = \dfrac{1}{m(\hat{K})}\displaystyle\int_{\hat{K}} \hat{u}$ for any $\hat{K} = \psi^{-1}(K)$.

Hence, we can state the following properties:

1. $\widehat{R_e^D}$ and $\widehat{R_e^C}$ are linear and continuous, respectively, on $H^2(\widehat{\Omega})$, and $H^1(\widehat{\Omega})$;
2. for $\hat{u}(\hat{x}) = u(\psi(\hat{x}))$, one can verify that

$$\widehat{R_e^D}(\hat{u}) \; = \; \bar{h}\, R_e^D(u), \quad \widehat{R_e^C}(\hat{u}) \; = \; R_e^C(u);$$

3. under assumptions 1 and 2 of Theorem 4.1, $\widehat{R_e^D}(\hat{u}) = 0$ for the linear functions $\hat{u}$, and $\widehat{R_e^C}(\hat{u}) = 0$ for the constant functions $\hat{u}$.

Using the lemma of Bramble and Hilbert, we deduce from points 1 and 3 that

$$\forall \hat{u} \in H^2(\widehat{\Omega}), \quad \left|\widehat{R_e^D}(\hat{u})\right| \; \leq \; c^D \; |\hat{u}|_{2,\,\widehat{\Omega}}\,, \quad \left|\widehat{R_e^C}(\hat{u})\right| \; \leq \; c^C \; |\hat{u}|_{1,\,\widehat{\Omega}}\,,$$

where $c^D$ and $c^C$ depends only on $\widehat{\Omega}$; and

$$|\hat{u}|_{m,\,\widehat{\Omega}} \; = \; \left(\sum_{|\alpha|=m} \|D^\alpha \hat{u}\|^2_{L^2(\widehat{\Omega})}\right)^{1/2}.$$

Finally, remark that

$$|\hat{u}|_{m,\,\widehat{\Omega}} \; = \; \bar{h}^{m-1} \; |u|_{m,\,\Omega_e} \quad (\text{for } \hat{u}(\hat{x}) \; = \; u(\psi(\hat{x}))).$$

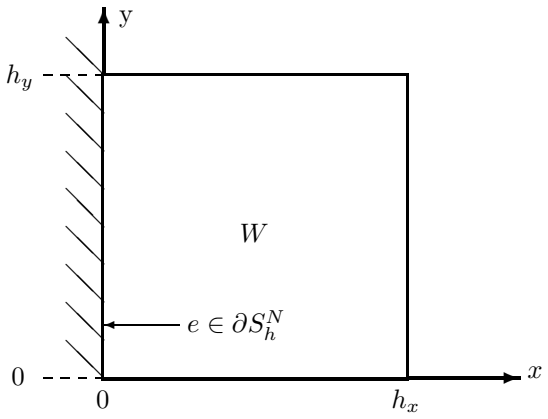


FIGURE 7. The Neumann boundary.

With point 2 above, we get

$$\forall u \in H^2(\Omega_e), \quad \left|R_e^D(u)\right| \leq c^D \, |u|_{2,\,\Omega_e}, \quad \left|R_e^C(u)\right| \leq c^C \, |u|_{1,\,\Omega_e}.$$

We recall that:

- $c = \max\left\{c^D, c^C\right\} > 0$ exists, because there are only a finite number of reference configurations;
- $R_e(u) = \nu R_e^D(u) + (\mathbf{v}\cdot\mathbf{n}_e)R_e^C(u)$;
- $h_e \leq h$, and $m(e) \leq h$,

and then,

$$|R_e(u)|^2 m(e) h_e \leq c^2(\nu + |\mathbf{v}|)^2 h^2 \|u\|^2_{H^2(\Omega_e)}.$$

**Second step.** Consider $e \in \partial S_h^N$. We only have to calculate $R_e^C(u) = \dfrac{1}{m(e)}\displaystyle\int_e u\mathrm{d}\sigma - \frac{1}{m(W)}\int_W u\mathrm{d}x$. The situation and the notations are described in Figure 7.

$$R_e^C(u) = \frac{1}{m(W)}\int_W (u(0,y) - u(x,y))\,\mathrm{d}x\mathrm{d}y.$$

A second order Taylor expansion yields (for $u \in C^2(\bar{W})$):

$$u(x,y) - u(0,y) = \partial_x u(0,y)\, x + \int_0^x \partial_{xx} u(s,y)(x-s)\,\mathrm{d}s.$$

After calculation, we find that

$$|R_e^C(u)|^2 m(e) \leq 2h^2\|k\|^2_{L^2(e)} + 2h^2\|u\|^2_{H^2(W)},$$

which is also true for $u \in H^2(W)$ by density of $C^2(\bar{W})$.

**Conclusion.** Since $N(K) = \mathrm{card}\,\{e \in S_h \mid K \in \Omega_e\}$ is uniformly bounded (by 12), we have

$$\sum_{e\in S_h\setminus\partial S_h^N} |R_e(u)|^2 m(e) h_e + \sum_{e\in\partial S_h^N} |R_e^C(u)|^2(\mathbf{v}\cdot\mathbf{n}_e)m(e) \leq ch^2\left(\|u\|^2_{H^2(\Omega)} + \|k\|^2_{L^2(\Gamma^N)}\right). \qquad \square$$

**Corollary 4.1** (Consistency of the weights of Fig. 5)**.** *The finite volume scheme described by the weights of Figure 5 is consistent.*

Remind that the weights are defined by approximating $u_h$ around a vertex by a linear function as close as possible to $u_h$. Consequently, the assumptions 1 and 2 of Theorem 4.1 are verified.

The scheme is naturally consistent along the boundary by construction (one can easily verify Assumptions 1 and 2).

### 4.3. **Coercivity**

Due to Lemma 3.1, we only have to prove that there exists a constant $c^\star$ such that for all $u_h$,

$$\left(\mathcal{L}_h^D u_h,\, u_h\right)_{L^2(\Omega)} \geq c^\star \sum_{e\in S_h\backslash\partial S_h^N} \left|\frac{u_E-u_W}{h_e}\right|^2 m(e)h_e,$$

where $\mathcal{L}_h^D u_h$ is calculated according to (5–8), with the boundary conditions $k=0$ and $g=0$ (see Sect. 2).

We recall that for any piecewise constant function $u_h$ [9,11], a discrete integration by parts yields

$$\left(\mathcal{L}_h^D u_h,\, u_h\right)_{L^2(\Omega)} \geq -\sum_{e\in S_h\backslash\partial S_h^N} \phi_e^D(u_h)\,\frac{u_E-u_W}{h_e}\,m(e)h_e = \sum_{e\in S_h\backslash\partial S_h^N} a_e(u_h,\, u_h). \tag{11}$$

**Remark 4.1.**

1. We consider only the sum for the $e\in S_h\backslash\partial S_h^N$, since $\phi_e^D(u_h)=0$ for $e\in\partial S_h^N$ (we just need the coercivity for discrete solutions of the homogeneous problem, $k=0$).
2. $\phi_e^D(u_h)$ is an approximation of $-\nu\nabla u_h\cdot\mathbf{n}_e$, while $u_E-u_W$ is an approximation of $\nabla u_h\cdot(x_E-x_W)$.
   - On the edges where $\alpha_e=0$, we have $a_e(u_h,\,u_h)=\nu\left|\frac{u_E-u_W}{h_e}\right|^2 m(e)h_e>0$.
   - On the edges where $\alpha_e\neq 0$, $u_h$ may be such that $a_e(u_h,\,u_h)<0$.

As a consequence, the natural decomposition of $a_h$ (11) on the edges $e$ does not permit to prove its coercivity, and *the difficulty appears only on the edges that have been refined*.

However, $a_h$ may also be decomposed as a summation of local bilinear operators $a_M$ on the vertices of the mesh.

Indeed, setting

$$u_e = \frac{h_e^W u_E + h_e^E u_W}{h_e} \quad (h_e^W=(x_N-x_W)\cdot\mathbf{n}_e,\; h_e^E=(x_E-x_N)\cdot\mathbf{n}_e),$$

the value linearly interpolated from $u_E$ and $u_W$ at the point $x_e$, intersection of $e$ and $[x_E,\,x_W]$ (Fig. 8), we can write, $\forall e\in S_h\backslash\partial S_h^N$,

$$\begin{aligned}
-\phi_e^D(u_h) &= \nu\left(\frac{u_E-u_W}{h_e}-\alpha_e\frac{u_N-u_S}{m(e)}\right)\\
&= \nu\left(\frac{u_E-u_W}{h_e}-\alpha_e\frac{u_N-u_e}{m(e^N)}\right)\frac{m(e^N)}{m(e)}+\nu\left(\frac{u_E-u_W}{h_e}-\alpha_e\frac{u_e-u_S}{m(e^S)}\right)\frac{m(e^S)}{m(e)},
\end{aligned}$$

where (Fig. 8)

$$m(e^N)=\mathrm{d}(x_e,\,x_N),\ \text{and}\ m(e^S)=\mathrm{d}(x_e,\,x_S).$$

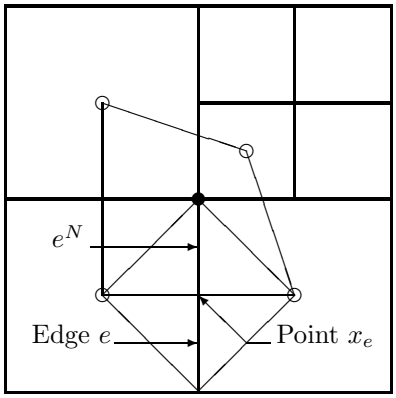


FIGURE 8. Notations around a vertex $M \in \mathcal{N}_h^\star$.

And then,

$$\begin{aligned} a_e(u_h,\, u_h) &= -\phi_e^D(u_h)\frac{u_E - u_W}{h_e}\, m(e)h_e \\ &= \nu\left(\frac{u_E - u_W}{h_e} - \alpha_e \frac{u_N - u_e}{m(e^N)}\right)\frac{u_E - u_W}{h_e}\, m(e^N)h_e \qquad (12) \\ &\quad + \nu\left(\frac{u_W - u_E}{h_e} - \alpha_e \frac{u_S - u_e}{m(e^S)}\right)\frac{u_W - u_E}{h_e} m(e^S)h_e \qquad (13) \\ &= a_e^N(u_h,\, u_h) + a_e^S(u_h,\, u_h). \end{aligned}$$

Remark that, if $e \in \partial S_h^D$, then we take $u_N = u_S = 0$ and $u_E = 0$ (resp. $u_W = 0$) if $\mathbf{n}_e = \mathbf{n}_{\rm ext}$ (resp. $\mathbf{n}_e = -\mathbf{n}_{\rm ext}$):

$$a_e^N(u_h,\, u_h) = \nu\left(\frac{u_E}{h_e}\right)^2 m(e^N)h_e, \quad a_e^S(u_h,\, u_h) = \nu\left(\frac{u_E}{h_e}\right)^2 m(e^S)h_e \quad (\text{case } \mathbf{n}_e = -\mathbf{n}_{\rm ext}),$$
$$a_e^N(u_h,\, u_h) = \nu\left(\frac{u_W}{h_e}\right)^2 m(e^N)h_e, \quad a_e^S(u_h,\, u_h) = \nu\left(\frac{u_W}{h_e}\right)^2 m(e^S)h_e \quad (\text{case } \mathbf{n}_e = \mathbf{n}_{\rm ext}).$$

(12) (resp. (13)) may only be used if $N \notin \partial\mathcal{N}_h^N$ – the Neumann Boundary – (resp. $S \notin \partial\mathcal{N}_h^N$); otherwise, we have, similarly (see (7) and (8)):

- if $M = N$ ($k_N = 0$, homogeneous boundary conditions),

$$\begin{aligned} a_e^N(u_h,\, u_h) &= \nu\left(\frac{u_E - u_W}{h_e} - \alpha_e \frac{|x_N - x_e|\, k_N}{m(e^N)}\right)\frac{u_E - u_W}{h_e}\, m(e^N)h_e \\ &= \nu\left|\frac{u_E - u_W}{h_e}\right|^2 m(e^N)h_e, \qquad (14) \end{aligned}$$

- if $M = S$ ($k_S = 0$),

$$\begin{aligned} a_e^S(u_h,\, u_h) &= \nu\left(\frac{u_E - u_W}{h_e} - \alpha_e \frac{|x_e - x_S|\, k_S}{m(e^S)}\right)\frac{u_E - u_W}{h_e}\, m(e^S)h_e \\ &= \nu\left|\frac{u_E - u_W}{h_e}\right|^2 m(e^S)h_e. \qquad (15) \end{aligned}$$

The contribution $a_e$ has been split into two parts $a_e^N$ *and* $a_e^S$*, that only depend on the geometry and on the values of* $u_h$*, respectively around the vertices* $x_N$*, and* $x_S$. As a consequence, we have proved the following result.

**Lemma 4.1** (Vertex decomposition of $a_h$)**.** *For all* $u_h$ *piecewise constant, we have*

$$\left(\mathcal{L}_h^D u_h,\, u_h\right)_{L^2(\Omega)} \geq \sum_{M\in\mathcal{N}_h} a_M(u_h,\, u_h),$$

*where* $a_M(u_h,\, u_h)$ *depends only on the geometry around* $M$ *and on the values of* $u_h$ *around* $M$ *(on the* $x_K$ *for* $K \in \mathcal{V}_M$*):*

$$a_M(u_h, u_h) \,=\, \nu \sum_{e\in S_h\setminus\partial S_h^N \,\mid\, M\in\bar{e}} a_e^M(u_h,\, u_h), \tag{16}$$

*and the* $a_e^M$ *are given by (14) and (15) if* $M$ *is on the Neumann boundary, and by (12) and (13) otherwise.*

**Remark 4.2** (The new, local, problem of coercivity)**.** For $M \in \mathcal{N}_h$, let

- $P_M^0$ be the space of the functions piecewise constant on the $K \in \mathcal{V}_M$ (remind that $\mathcal{V}_M$ is the neighborhood of $M$).

We have to prove that, for all $M \in \mathcal{N}_h$, the local bilinear operator $a_M$ defined on $P_M^0$ verifies:

$$a_M(u_h,\, u_h) \,\geq\, \alpha_h(M)\,[u_h]_{1,M}^2,$$

where

$$[u_h]_{1,M}^2 \,=\, \sum_{e\in S_h\setminus\partial S_h^N \,\mid\, M\in\bar{e}} \left|\frac{u_E - u_W}{h_e}\right|^2 m(e^M)h_e; \tag{17}$$

and to find a lower bound on the $\alpha_h(M)$, uniform with respect to $h$.

Remark that

$$\sum_{M\in\mathcal{N}_h} [u_h]_{1,M}^2 = \sum_{e\in S_h\setminus\partial S_h^N} \left|\frac{u_E - u_W}{h_e}\right|^2 m(e)h_e.$$

This problem

- is local around each vertex of the mesh;
- depends on the eigenvalues of the matrix of $a_M$, of size $n_M$, the number of neighbors of the vertex $M$.

Concerning the uniformity with respect to $h$, we have the following result.

**Lemma 4.2** ($h$-uniformity)**.** *For any* $M \in \mathcal{N}_h$*, there exists* $h$ *such that*

- $x = \psi_h(\hat{x}) = x_M + h\hat{x}$ *maps the geometry around* $M$ *onto the geometry of one of the reference neighborhoods of Figure 9 (we shall add a* $\widehat{\ }$ *to the previous notations when considering the image by* $\psi_h^{-1}$ *of the actual geometry).*

*For any function* $u_h \in P_M^0$ *(piecewise constant, defined on the* $x_K$ *for* $K \in \mathcal{V}_M$*), let* $\widehat{u} = u_h \circ \psi_h$ *be the function defined on the* $\widehat{x_K}$ *for* $\widehat{K} \in \widehat{\mathcal{V}_M}$*, by* $u_h(x) = \hat{u}(\hat{x})$.

*For any* $\alpha > 0$*, we have*

$$\forall u_h \text{ defined on the } x_K\,(K\in\mathcal{V}_M), \quad a_M(u_h,\, u_h) \geq \alpha\,[u_h]_{1,M}^2 \Leftrightarrow \widehat{a_M}(\hat{u},\, \hat{u}) \geq \alpha\,[\hat{u}]_{1,\widehat{M}}^2,$$

*where* $\widehat{a_M}(\hat{u},\, \hat{u})$ *is given by formulae (12–15), but for the* $\widehat{\ }$ *geometry and the function* $\hat{u}$.

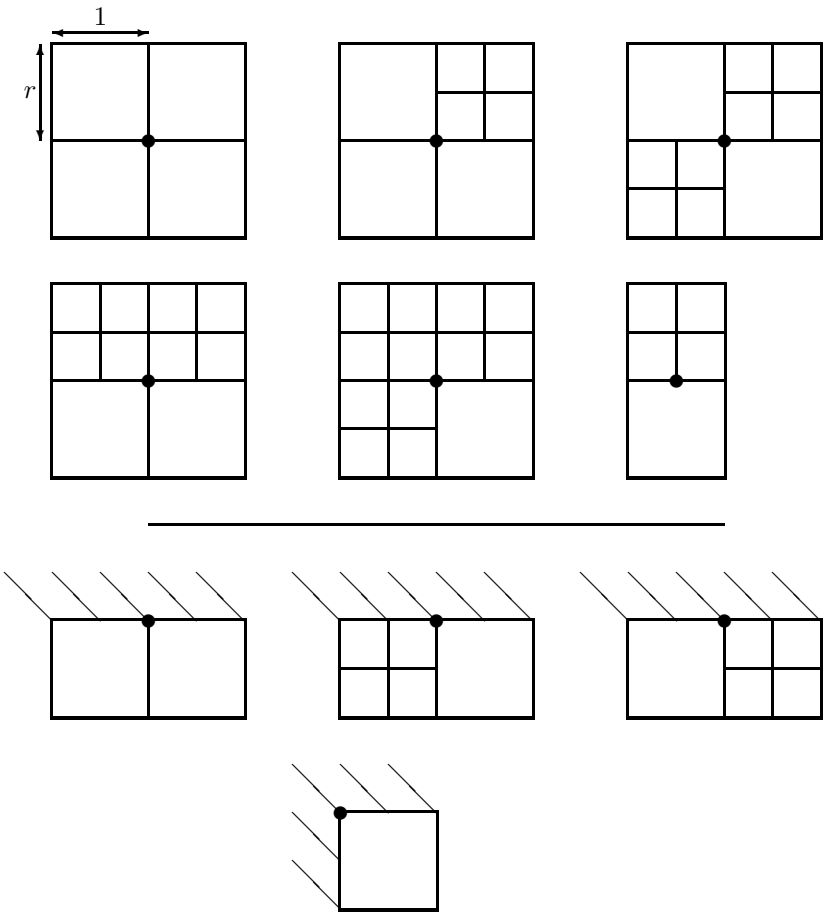


FIGURE 9. Interior and boundary reference cases.

*Proof.* Suppose that $M \in \mathcal{N}_h$, and $\hat{u}$ is piecewise constant of values $\hat{u}_K$ for $\widehat{K} \in \widehat{\mathcal{V}_M}$. We always have:

1. $u_K = \hat{u}_{\widehat{K}}$, for any $K \in \mathcal{V}_M$;
2. $\hat{u}_M = \sum_{\widehat{K} \in \widehat{\mathcal{V}_M}} y_K(M) \hat{u}_K = \sum_{K \in \mathcal{V}_M} y_K(M) u_K = u_M$ if $M \in \mathcal{N}_h^\star$ (the interior vertices);
3. $\hat{u}_M = u_M = 0$ if $M \in \partial\mathcal{N}_h^D$ (homogeneous boundary condition);
4. $h_e = h\,\widehat{h_e}$, and $m(e^M) = h\, m(\widehat{e^M})$, and $\alpha_e = \widehat{\alpha_e}$, for any $e \in S_h \backslash \partial S_h^N$ such that $M \in \bar{e}$.

As a consequence, we naturally have (formulae (12–15) and (17)):

$$a_e^M(u_h, u_h) = \widehat{a_e^M}(\hat{u}, \hat{u}), \quad [u_h]_{1,M} = [\hat{u}]_{1,\hat{M}},$$

which completes the proof. □

## 5. Analysis of the coercivity

At last, we shall analyze the operators $\widehat{a_M}$ in the different reference cases of Figure 9 (see Rem. 4.2). Therefore, remark that, in each case, $[\cdot]_{1,\hat{M}}$ is a norm on the space $P^0_{\widehat{M}}$ of the functions piecewise constant, modulo the functions constant on $\mathcal{V}_{\widehat{M}}$.

**Lemma 5.1** (Condition of coercivity)**.** *Suppose that, in any of the cases listed in Figure 9, $\widehat{a_M}$ is positive definite on $P^0_{\widehat{M}}$, modulo the constant functions; then, there exist $c^\star > 0$ (independent of $h$, Lem. 4.2) such that*

$$\forall u_h, \quad a_h(u_h, u_h) \geq c^\star \, |u_h|^2_{1,h}.$$

*Proof.* Indeed, under the assumption above, such a constant exists in any of the reference cases:

$$\forall \hat{u} \in P^0_{\widehat{M}}, \quad \widehat{a_M}(\hat{u}, \hat{u}) \geq c_{\widehat{M}} \, [\hat{u}]^2_{1,\widehat{M}}$$

(because $\dim P^0_{\widehat{M}} < +\infty$), and then $c^\star$ is the minimum of them. □

The local positivity is analyzed below for each reference case. As a matter of fact, we shall see that:

**Theorem 5.1** (Sufficient condition of coercivity of the scheme)**.** *If*

$$\frac{1}{r} < \frac{\Delta y}{\Delta x} < r, \quad \textit{where } r = 3 + 2\sqrt{2},$$

*then the scheme defined by (3) to (8), and the weights of Figure 5 is coercive.*

In the following sections, we drop the $\widehat{\ }$, as well as the index $h$ in the notations, since we deal with the reference cases.

## 5.1. The Neumann boundary

Consider a function $u$, *piecewise constant on the* $K \in \mathcal{V}_M$, where $M \in \partial\mathcal{N}^N$ (the Neumann boundary):

- on the unique interior edge $e$ such that $M \in \bar{e}$, we have seen that (see (14) and (15))

$$a^M_e(u, u) = \nu \left| \frac{u_E - u_W}{h_e} \right|^2 m(e^M) h_e;$$

- the two edges $e$ of the Neumann boundary are not taken into account in the expression of $a_M(u, u)$ (16), nor in the expression of $[u]_{1,M}$ (17). As a matter of fact, we have $\phi^D_e(u) = 0$ (homogeneous boundary condition and (6)), and then $a^M_e(u, u) = 0$ on theses edges.

Consequently,

$$a_M(u, u) = \nu [u]^2_{1,M}.$$

## 5.2. The Dirichlet boundary

Consider a function $u$, *piecewise constant on the* $K \in \mathcal{V}_M$, where $M \in \partial\mathcal{N}^D$ (the Dirichlet boundary).

### 5.2.1. *First cases*

In both cases of Figure 10, the edges $e$ such that $M \in \bar{e}$ verify $\alpha_e = 0$ (no refinement). As a consequence, there are no contributions $u_N - u_S$ in $\phi^D_e$, and then

$$\widehat{a_M}(u, u) = \nu \, [u]^2_{1,M}.$$

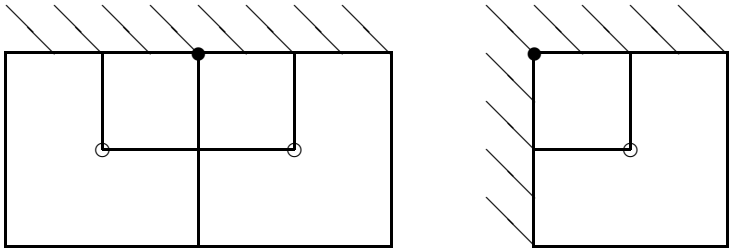

FIGURE 10. Dirichlet boundary.

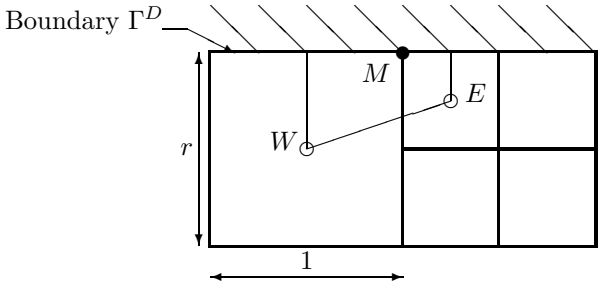


FIGURE 11. Dirichlet boundary.

5.2.2. *Second case*

In Figure 11, $r$ represents the aspect ratio of the reference figure, which may be either $\Delta x/\Delta y$, or $\Delta y/\Delta x$. We calculate $a_M(u,\, u)$ with formulae (12) and (13), assuming that $u = 0$ on $\Gamma^D$:

$$\begin{aligned}\frac{1}{\nu}\widehat{a_M}(u,\, u) &= \left(\frac{u_W - 0}{r/2}\right)^2 \frac{r}{2}\frac{1}{2} + \left(\frac{u_E - 0}{r/4}\right)^2 \frac{r}{4}\frac{1}{4} + \left(\frac{u_E - u_W}{3/4} - \frac{r}{3}\frac{0 - (u_W/3 + 2u_E/3)}{r/3}\right)\frac{u_E - u_W}{3/4}\frac{3}{4}\frac{r}{3} \\ &= \begin{bmatrix} u_W & u_E \end{bmatrix} \mathcal{M}_M \begin{bmatrix} u_W \\ u_E \end{bmatrix},\end{aligned}$$

with

$$\mathcal{M}_M = \begin{bmatrix} \dfrac{1}{r} + \dfrac{1}{3}r & -\dfrac{1}{2}r \\ -\dfrac{1}{2}r & \dfrac{1}{r} + \dfrac{2}{3}r \end{bmatrix}, \text{ and we have } \det\mathcal{M}_M = \frac{1}{36}\frac{1}{r^2}\left(36 + 36r^2 - r^4\right).$$

5.2.3. *Third case*

A similar calculation (swapping $u_E$ and $u_W$, and replacing $\alpha_e = +r/3$ by $\alpha_e = -r/3$) yields, in that case:

$$\mathcal{M}_M = \begin{bmatrix} \dfrac{1}{r} + \dfrac{2}{3}r & -\dfrac{1}{2}r \\ -\dfrac{1}{2}r & \dfrac{1}{r} + \dfrac{1}{3}r \end{bmatrix}, \text{ and we have } \det\mathcal{M}_M = \frac{1}{36}\frac{1}{r^2}\left(36 + 36r^2 - r^4\right).$$

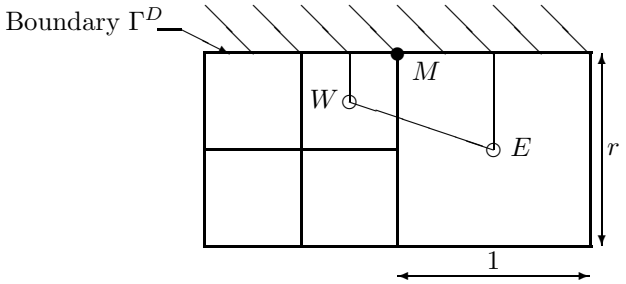


FIGURE 12. Dirichlet boundary.

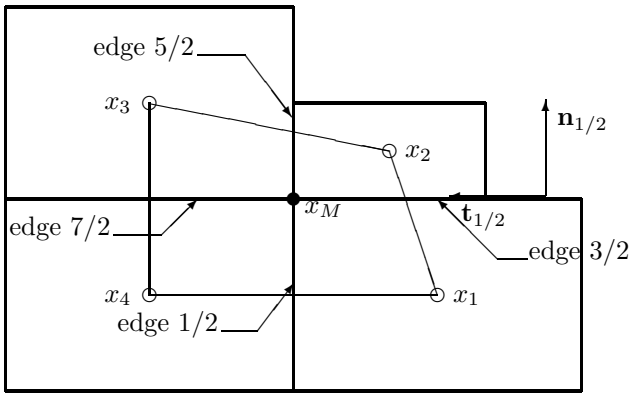


FIGURE 13. Generalized interior case.

In both those cases, $\widehat{a_M}$ is definite positive if

$$\det \mathcal{M}_M > 0 \Leftrightarrow 0 \leq r^2 < 18 + 6\sqrt{10}.$$

Since $r$ represents either the ratio $\Delta x/\Delta y$, or the ratio $\Delta y/\Delta x$, *the final condition of coercivity on the Dirichlet boundary is*

$$\frac{1}{r_0} < \frac{\Delta x}{\Delta y} < r_0, \quad \text{with } r_0 = \sqrt{18 + 6\sqrt{10}}.$$

## 5.3. **Interior cases**

Suppose that $M \in \mathcal{N}^\star$ is an interior vertex.

Remark in Figure 9 that there are three (one case) or four (five cases) control volumes around such a vertex $M$. Hence, *the matrix of* $a_M$ *is of size* $3 \times 3$ *or* $4 \times 4$, and it can be calculated.

### 5.3.1. *Introduction*

It order to simplify these calculations, we introduce some notations.

Consider the example of Figure 13: the edges and the cells are ordered and oriented by the trigonometric direction.

Given $u \in P_M^0$, piecewise constant, of value $u_i$ at $x_i$, consider the function $\tilde{u}$, piecewise linear on the triangles $T_{i+1/2} = (x_M, x_i, x_{i+1})$, such that

$$\tilde{u}(x_M) = u_M, \text{ and } \forall i, \tilde{u}(x_i) = u_i.$$

We can write $\tilde{a}_M(\tilde{u}, \tilde{u}) = a_M(u, u)$ the bilinear operator for the functions $\tilde{u}$.

Remark that

$$\forall i, \quad \frac{u_{i+1} - u_i}{h_{i+1/2}} = \nabla \tilde{u}_{i+1/2} \cdot (\mathbf{n} + \alpha \mathbf{t})_{i+1/2}, \text{ and } \phi_i^D(u) = -\nu \nabla \tilde{u}_{i+1/2} \cdot \mathbf{n}_{i+1/2},$$

and that $m(e_{i+1/2}) h_{i+1/2} = 2m(T_{i+1/2})$.

Consequently, we have

$$\tilde{a}_M(\tilde{u}, \tilde{u}) = a_M(u, u) = 2\nu \sum_i {}^{\mathrm{t}}\nabla \tilde{u}_{i+1/2} \, \mathcal{S}_{i+1/2} \nabla \tilde{u}_{i+1/2} \, m(T_{i+1/2}), \tag{18}$$

where $\mathcal{S}_{i+1/2}$ is the symmetric part of $(\mathbf{n} + \alpha \mathbf{t})_{i+1/2} \, {}^{\mathrm{t}}\mathbf{n}_{i+1/2}$:

$$\mathcal{S}_{i+1/2} = \frac{1}{2} \left( (\mathbf{n} + \alpha \mathbf{t})_{i+1/2} \, {}^{\mathrm{t}}\mathbf{n}_{i+1/2} + \mathbf{n}_{i+1/2} \, {}^{\mathrm{t}}(\mathbf{n} + \alpha \mathbf{t})_{i+1/2} \right).$$

5.3.2. *A basis to calculate the matrix of $a_M$*

Here is now the argument that leads to a more easy calculation of the matrices $a_M$ in the different cases. The details may be found in [9].

1. The function $\mathbb{1}(x) = 1$, constant on $\mathcal{V}_M$, belongs to the kernel of $a_M$, because the flux of diffusion $\phi^D_{i+1/2}(\mathbb{1}) = 0$ on any edge:

$$a_M(\mathbb{1}, u) = 0, \quad \forall u.$$

2. Consider the piecewise constant functions

$$u^1(x) = x_i^1, \quad \forall x \in K_i, \quad u^2(x) = x_i^2, \quad \forall x \in K_i,$$

where $x_i = (x_i^1, x_i^2)$ $(i = 1 \dots n)$ are the centers of the $K_i \in \mathcal{V}_M$. Since the construction of $u_M$ is exact for the linear functions, the function $\tilde{u}^k$ associated to $u^k$ is

$$\tilde{u}^k(x) = x^k, \text{ which verifies } \nabla \tilde{u}^1(x) = \begin{bmatrix} 1 \\ 0 \end{bmatrix}, \quad \nabla \tilde{u}^2(x) = \begin{bmatrix} 0 \\ 1 \end{bmatrix}.$$

As a consequence, using (18), we have

$$a_M(u^k, u^l) = 2\nu \, s_{kl}, \quad \text{where } \mathcal{S}_M = (s_{kl}) = \sum_i \mathcal{S}_{i+1/2} m(T_{i+1/2}).$$

3. Suppose that $u^3$ is any function such that $(\mathbb{1}, u^1, u^2, u^3)$ is a basis of $P_M^0$, then,

$$\text{the matrix } B \text{ of } a_M \text{ in the basis } (\mathbb{1}, u^1, u^2, u^3) \text{ is } B = \begin{bmatrix} 0 & 0 & 0 \\ 0 & \mathcal{S}_M & \star \\ 0 & \star & \star \end{bmatrix}.$$

4. Remark that we may choose the axes of coordinates for $(x^1, x^2)$ in order that $\mathcal{S}_M$ is diagonal; and then the matrix $B$ is simply:

$$B = \begin{bmatrix} 0 & 0 & 0 & 0 \\ 0 & s_{11} & 0 & b_{24} \\ 0 & 0 & s_{22} & b_{34} \\ 0 & b_{24} & b_{34} & b_{44} \end{bmatrix}.$$

5. At last, $B$ is positive definite modulo the constant functions (which is the space $\mathbb{R}\mathbb{1}$) if

$$s_{11} > 0, \quad s_{22} > 0, \quad b_{44} > 0, \quad \det \begin{bmatrix} s_{11} & 0 & b_{24} \\ 0 & s_{22} & b_{34} \\ b_{24} & b_{34} & b_{44} \end{bmatrix} > 0.$$

6. If $M$ is only surrounded by three control volumes, $\dim P^0_M = 3$, and we conclude directly from point 2, that $(\mathbb{1}, u^1, u^2)$ is a basis in which the matrix $B$ of $a_M$ is

$$B = \begin{bmatrix} 0 & 0 & 0 \\ 0 & s_{11} & 0 \\ 0 & 0 & s_{22} \end{bmatrix}.$$

**Remark 5.1.**

- $\mathcal{S}_{i+1/2}$ is an indicator of the difference between the direction $x_i$, $x_{i+1}$ and the direction $\mathbf{n}_{i+1/2}$. Hence, $\mathcal{S}_M$ is the average of this indicator on all the edges surrounding the vertex $M$.
- It follows from point 3 that the intuitive condition

  $\mathcal{S}_M$ *is definite positive,*

  is *a necessary condition of coercivity of* $a_M$ (if $M$ is surrounded by three control volumes, it is also a sufficient condition).

5.3.3. *Local conditions of coercivity, case by case*

Practically, we calculate the matrices of the $a_M$ in the canonical basis of the functions

$$v_i(x) = 1 \text{ if } x \in K_i, \quad v_i(x) = 0 \text{ otherwise},$$

because it is quite easy; and then $u_3$ is chosen to be a vector perpendicular to $(\mathbb{1}, u^1, u^2)$ for the canonical inner product. Consequently, we can change of coordinates from the canonical basis to the basis $(\mathbb{1}, u^1, u^2, u^3)$ by using matrix

$$P = \begin{bmatrix} 1 & x_1^1 & x_1^2 & t_1 \\ 1 & x_2^1 & x_2^2 & t_2 \\ 1 & x_3^1 & x_3^2 & t_3 \\ 1 & x_4^1 & x_4^2 & t_4 \end{bmatrix},$$

where $x_i = (x_i^1, x_i^2)$ are the coordinates of center $x_i$, and $u^3 = (t_1, \ldots, t_4)$ belongs to the orthogonal of $\{\mathbb{1}, u^1, u^2\}$ for the canonical inner product.

The reference geometrical cases studied below are presented with the aspect ratio $r$, which may represent either $\Delta y/\Delta x$, or $\Delta y/\Delta x$. The conditions of point 5 above, of the form $r > r_i$, or $r < r_j$, yields that *the*

*condition of coercivity is always*

$$\frac{1}{r_i} < \frac{\Delta y}{\Delta x} < r_i.$$

The geometries and the corresponding $r_i$ are displayed below.

1. No refinement

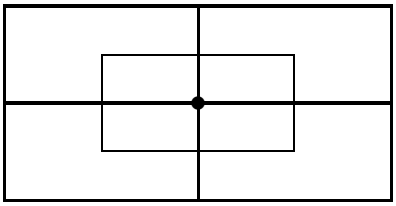

The result does not need any calculation: in that case, the angle $\alpha$ is equal to 0 on any edge, and then

$$\forall u, \quad a_M(u, u) = [u]^2_{1,M}.$$

2. One refinement

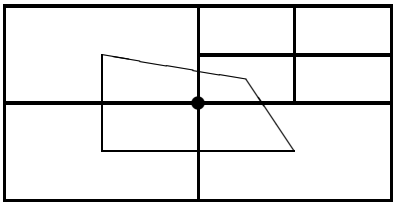

The condition of positivity of the matrix $B$ is:

$$18r - 1 - r^2 > 0,$$
$$\det B = \frac{64r^4 - 6193r^2 + 64}{r^2 - 18r + 1} > 0.$$

We find:

$$r_1 = 9 + 4\sqrt{5}, \quad r_2 = \sqrt{\frac{6193 + 7\sqrt{782385}}{128}}.$$

3. Two consecutive control volumes are refined

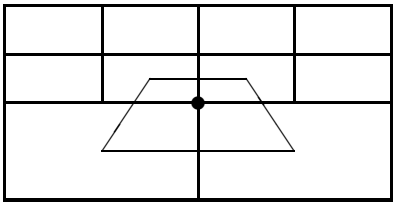

The condition of positivity of the matrix $B$ is:

$$\det B = 36r^4 + 36r^2 - 1 > 0.$$

We find:

$$r_3 = \sqrt{18 + 6\sqrt{10}}.$$

4. Two opposite control volumes are refined

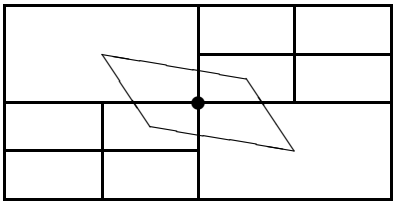

The condition of positivity of the matrix $B$ is:

$$6r - 1 - r^2 > 0.$$

We find:

$$r_4 = 3 + 2\sqrt{2}.$$

5. Three control volumes are refined

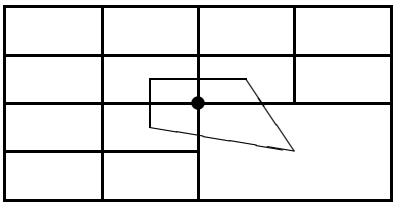

The condition of positivity of the matrix $B$ is:

$$9r - 1 - r^2 > 0,$$
$$\det B = \frac{121r^4 - 6010r^2 + 121}{r^2 - 9r + 1} > 0.$$

We find:

$$r_5 = \frac{9+\sqrt{77}}{2}, \quad r_6 = \sqrt{\frac{3005 + 2\sqrt{2253846}}{121}}.$$

6. Three control volumes around $M$

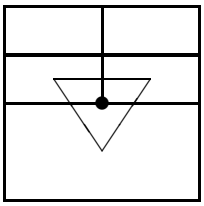

The matrix $\mathcal{S}_M$ is definite positive, and then, the scheme is unconditionally coercive in this case.

5.3.4. *Matrices of $aM$, case by case*

Here are the matrices $B$, of $a_M$ in the basis $(X^1, X^2, X^3)$, corresponding to the six cases above.

1. No control volume is refined

$$B = \begin{bmatrix} 4r & 0 & 0 \\ 0 & 4r & 0 \\ 0 & 0 & 4\dfrac{1+r^2}{r} \end{bmatrix}.$$

2. One control volume is refined

$$B = \begin{bmatrix} 3r - \dfrac{1}{6} - \dfrac{1}{6}r^2 & 0 & \dfrac{\sqrt{2}}{72}\dfrac{-r^2+11+11r^3-r}{r} \\ 0 & 3r + \dfrac{1}{6} + \dfrac{1}{6}r^2 & \dfrac{\sqrt{2}}{72}\dfrac{r^2-11+11r^3-r}{r} \\ \dfrac{\sqrt{2}}{72}\dfrac{-r^2+11+11r^3-r}{r} & \dfrac{\sqrt{2}}{72}\dfrac{r^2-11+11r^3-r}{r} & \dfrac{229}{54}\dfrac{r^2+1}{r} \end{bmatrix}.$$

3. Two consecutive control volumes are refined

$$B = \begin{bmatrix} \dfrac{5}{2}r & 0 & -\dfrac{5}{6}\dfrac{1}{r} \\ 0 & 2r & 0 \\ -\dfrac{5}{6}\dfrac{1}{r} & 0 & 10\dfrac{1+r^2}{r} \end{bmatrix}.$$

4. Two opposite control volumes are refined

$$B = \begin{bmatrix} 2r - \frac{1}{3} - \frac{1}{3}r^2 & 0 & 0 \\ 0 & 2r + \frac{1}{3} + \frac{1}{3}r^2 & 0 \\ 0 & 0 & 4\frac{1+r^2}{r} \end{bmatrix}.$$

5. Three control volumes are refined

$$B = \begin{bmatrix} \frac{3}{2}r - \frac{1}{6} - \frac{1}{6}r^2 & 0 & -\frac{\sqrt{2}}{24}\frac{-r^2+4r^3+r-4}{r} \\ 0 & \frac{3}{2}r + \frac{1}{6} + \frac{1}{6}r^2 & -\frac{\sqrt{2}}{24}\frac{r+4+4r^3+r^2}{r} \\ -\frac{\sqrt{2}}{24}\frac{-r^2+4r^3+r-4}{r} & -\frac{\sqrt{2}}{24}\frac{r+4+4r^3+r^2}{r} & \frac{227}{24}\frac{1+r^2}{r} \end{bmatrix}.$$

6. Three control volumes around $M$

$$B = \begin{bmatrix} \frac{1}{2}r & 0 \\ 0 & r \end{bmatrix}.$$

5.3.5. *Classification of the cases*

At last, the different geometries can be classified from the most to the less limitative one. We have

$$3 + 2\sqrt{2} = r_4 < r_0 = r_3 < r_6 < r_2.$$

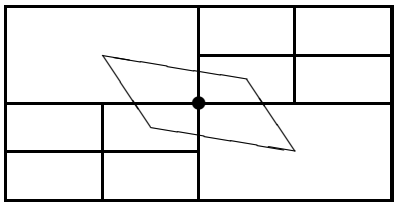

$$r_4 = 3 + 2\sqrt{2} \sim 5.83.$$

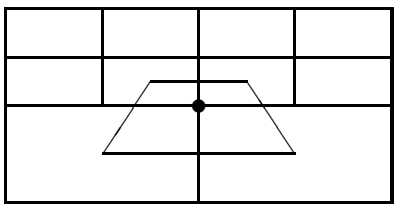

$$r_3 = \sqrt{18 + 6\sqrt{10}} \sim 6.08.$$

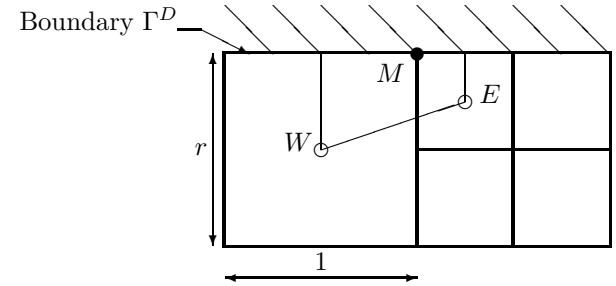


$$r_0 = \sqrt{18 + 6\sqrt{10}} \sim 6.08.$$

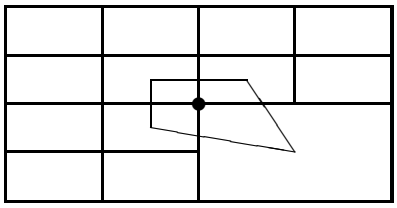

$$r_6 = \sqrt{\frac{3005 + 2\sqrt{2253846}}{121}} \sim 7.05.$$

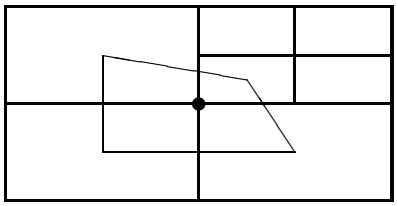

$$r_2 = \sqrt{\frac{6193 + 7\sqrt{782385}}{128}} \sim 9.84.$$

## References


[1] R.E. Bank and D.J. Rose, Some error estimates for the box method. *SIAM J. Numer. Anal.* **24** (1987) 777–787.

[2] J. Baranger, J.F. Maitre and F. Oudin, Connection between finite volume and mixed finite element methods. *RAIRO Modél. Math. Anal. Numér.* **30** (1996) 445–465.

[3] M.J. Berger and P. Collela, Local adaptative mesh refinement for shock hydrodynamics. *J. Comput. Phys.* **82** (1989) 64–84.

[4] Z. Cai, On the finite volume element method. *Numer. Math.* **58** (1991) 713–735.

[5] Z. Cai, J. Mandel and S. McCormick, The finite volume element method for diffusion equations on general triangulations. *SIAM J. Numer. Anal.* **28** (1991) 392–402.

[6] Z. Cai and S. McCormick, On the accuracy of the finite volume element method for diffusion equations on composite grids. *SIAM J. Numer. Anal.* **27** (1990) 636–655.

[7] W.J. Coirier, *An Adaptatively-Refined, Cartesian, Cell-based Scheme for the Euler and Navier-Stokes Equations*. Ph.D. thesis, Michigan Univ., NASA Lewis Research Center (1994).

[8] W.J. Coirier and K.G. Powell, A Cartesian, cell-based approach for adaptative-refined solutions of the Euler and Navier-Stokes equations. *AIAA* (1995).

[9] Y. Coudière, *Analyse de schémas volumes finis sur maillages non structurés pour des problèmes linéaires hyperboliques et elliptiques*. Ph.D. thesis, Université Paul Sabatier (1999).

[10] Y. Coudière, T. Gallouët and R. Herbin, Discrete sobolev inequalities and $l^p$ error estimates for approximate finite volume solutions of convection diffusion equation. Preprint of LATP, University of Marseille 1, 98-13 (1998).

[11] Y. Coudière, J.P. Vila and P. Villedieu, Convergence rate of a finite volume scheme for a two dimensionnal diffusion convection problem. *ESAIM: M2AN* **33** (1999) 493–516.

[12] B. Courbet and J.P. Croisille, Finite volume box schemes on triangular meshes. *RAIRO Modél. Math. Anal. Numér.* **32** (1998) 631–649.

[13] M. Dauge, Elliptic Boundary Value Problems in Corner Domains. *Lect. Notes Math.*, Springer-Verlag, Berlin (1988).

[14] R.E. Ewing, R.D. Lazarov and P.S. Vassilevski, Local refinement techniques for elliptic problems on cell-centered grids. I. Error analysis. *Math. Comp.* **56** (1991) 437–461.

[15] R. Eymard, T. Gallouët and R. Herbin, Finite volume methods, in *Handbook of Numerical Analysis*, P.G. Ciarlet and J.L. Lions Eds. (to appear). Prépublication No 97-19 du LATP, UMR 6632, Marseille (1997).

[16] P.A. Forsyth and P.H. Sammon, Quadratic convergence for cell-centered grids. *Appl. Numer. Math.* **4** (1988) 377–394.

[17] B. Heinrich, Finite Difference Methods on Irregular Networks. *Internat. Ser. Numer. Anal.* **82**, Birkhaüser, Verlag Basel (1987).

[18] R. Herbin, An error estimate for a finite volume scheme for a diffusion-convection problem on a triangular mesh. *Numer. Methods Partial Differential Equations* **11** (1994) 165–173.
[19] F. Jacon and D. Knight, A Navier-Stokes algorithm for turbulent flows using an unstructured grid and flux difference splitting. *AIAA* (1994).
[20] H. Jianguo and X. Shitong, On the finite volume element method for general self-adjoint elliptic problem. *SIAM J. Numer. Anal.* **35** (1998) 1762–1774.
[21] P. Lesaint, Sur la résolution des systèmes hyperboliques du premier ordre par des méthodes d'éléments finis. Technical report, CEA (1976).
[22] T.A. Manteuffel and A.B. White, The numerical solution of second-order boundary values problems on nonuniform meshes. *Math. Comp.* **47** (1986) 511–535.
[23] K. Mer, Variational analysis of a mixed finite element finite volume scheme on general triangulations. Technical Report 2213, INRIA, Sophia Antipolis (1994).
[24] I.D. Mishev, Finite volume methods on voronoï meshes. *Numer. Methods Partial Differential Equations* **14** (1998) 193–212.
[25] K.W. Morton and E. Süli, Finite volume methods and their analysis. *IMA J. Numer. Anal.* **11** (1991) 241–260.
[26] E. Süli, Convergence of finite volume schemes for Poisson's equation on nonuniform meshes. *SIAM J. Numer. Anal.* **28** (1991) 1419–1430.
[27] J.-M. Thomas and D. Trujillo. Analysis of finite volumes methods. Technical Report 95/19, CNRS, URA 1204 (1995).
[28] J.-M. Thomas and D. Trujillo, Convergence of finite volumes methods. Technical Report 95/20, CNRS, URA 1204 (1995).
[29] R. Vanselow and H.P. Scheffler, Convergence analysis of a finite volume method *via* a new nonconforming finite element method. *Numer. Methods Partial Differential Equations* **14** (1998) 213–231.
[30] P.S. Vassilevski, S.I. Petrova and R.D. Lazarov. Finite difference schemes on triangular cell-centered grids with local refinement. *SIAM J. Sci. Stat. Comput.* **13** (1992) 1287–1313.
[31] A. Weiser and M.F. Wheeler, On convergence of block-centered finite differences for elliptic problems. *SIAM J. Numer. Anal.* **25** (1988) 351–375.